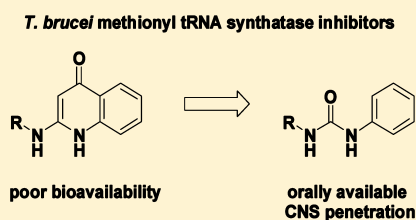


Urea-Based Inhibitors of *Trypanosoma brucei* Methionyl-tRNA Synthetase: Selectivity and in Vivo CharacterizationSayaka Shibata,<sup>†,‡</sup> J. Robert Gillespie,<sup>§</sup> Ranae M. Ranade,<sup>§</sup> Cho Yeow Koh,<sup>†</sup> Jessica E. Kim,<sup>†</sup> Joy U. Laydbak,<sup>§</sup> Frank H. Zucker,<sup>†</sup> Wim G. J. Hol,<sup>†</sup> Christophe L. M. J. Verlinde,<sup>†</sup> Frederick S. Buckner,<sup>\*,§</sup> and Erkang Fan<sup>\*,†</sup><sup>†</sup>Department of Biochemistry, <sup>‡</sup>Department of Chemistry, and <sup>§</sup>Department of Medicine, University of Washington, Seattle, Washington 98195, United States

## S Supporting Information

**ABSTRACT:** Urea-based methionyl-tRNA synthetase inhibitors were designed, synthesized, and evaluated for their potential toward treating human African trypanosomiasis (HAT). With the aid of a homology model and a structure–activity–relationship approach, low nM inhibitors were discovered that show high selectivity toward the parasite enzyme over the closest human homologue. These compounds inhibit parasite growth with EC<sub>50</sub> values as low as 0.15 μM while having low toxicity to mammalian cells. Two compounds (**2** and **26**) showed excellent membrane permeation in the MDR1-MDCKII model and encouraging oral pharmacokinetic properties in mice. Compound **2** was confirmed to enter the CNS in mice. Compound **26** had modest suppressive activity against *Trypanosoma brucei rhodesiense* in the mouse model, suggesting that more potent analogues or compounds with higher exposures need to be developed. The urea-based inhibitors are thus a promising starting point for further optimization toward the discovery of orally available and CNS active drugs to treat HAT.



## ■ INTRODUCTION

Approximately 60 million people in sub-Saharan Africa are at risk for human African trypanosomiasis (HAT) caused by *Trypanosoma brucei*. HAT caused by *Trypanosoma brucei gambiense* progresses slowly from early stage to late stage disease, whereas disease caused by *Trypanosoma brucei rhodesiense* progresses rapidly.<sup>1,2</sup> In late stage HAT, the central nervous system (CNS) becomes infected and the untreated disease is uniformly fatal. Depending on the stage of the disease and the subspecies of the causative agent, HAT is treated either with suramin, pentamidine, melarsoprol, eflornithine, or a combination of nifurtimox and eflornithine.<sup>1,2</sup> These currently used drugs are either highly toxic and/or need to be administered by injection. Thus, there is an urgent need to develop new therapeutics that are effective, safe, affordable, orally administered, and easily stored in tropical conditions (<http://www.dndi.org/diseases/hat/target-product-profile.html>).

Methionyl-tRNA synthetase (MetRS), as one of the aminoacyl-tRNA synthetases (aaRS), plays an essential role in the core biological process of translating nucleotide-encoded gene sequences into proteins. The enzymatic reaction of aaRS generally consists of the following steps: the recognition of a specific amino acid and ATP, the formation of an aminoacyl-adenylate, the recognition of a specific tRNA, and the transfer of the aminoacyl group to the 3'-end of the tRNA.<sup>3</sup> We recently showed by RNAi knockdown that the single MetRS of *T. brucei* is essential for parasite survival.<sup>4</sup> Moreover, we synthesized a series of potent aminoquinolone-based inhibitors of parasite MetRS that inhibited parasite growth in culture, further

demonstrating that MetRS is an attractive protein drug target for *T. brucei*.<sup>4</sup> However, aminoquinolone-based MetRS inhibitors were known from antibacterial work to have poor bioavailability.<sup>5,6</sup> In our own hands, this series of compounds indeed exhibited poor permeability in the MDR1-MDCKII model that predicts CNS penetration,<sup>7–9</sup> making it unlikely that they would cross the blood–brain barrier for treating late stage HAT. These pharmacokinetic (PK) liabilities prompted us to explore other scaffolds to block *T. brucei* MetRS in our investigations toward anti-HAT therapeutics. In this paper, we report that using a urea moiety to replace the aminoquinolone group resulted in selective MetRS inhibitors that show good potency in parasite growth inhibition assays and promising improvements in bioavailability.

## ■ RESULTS AND DISCUSSION

**Design of Urea-Based Inhibitors.** The starting point for the work in this paper is the predicted binding mode of aminoquinolone-based compound **1** in a homology model of *T. brucei* MetRS that we reported earlier.<sup>4</sup> We were able to create a high quality model because of the disclosure in a conference poster by the Replidyne company of a cocrystal structure of a related aminoquinolone-based inhibitor bound to *Clostridium difficile* MetRS.<sup>10</sup> Compound **1** was successfully docked into the model, filling two binding pockets. The benzyl fragment occupies the mostly hydrophobic methionine substrate pocket, and one of the *meta*-chlorine atoms resides essentially in the

Received: March 2, 2012

Published: June 21, 2012

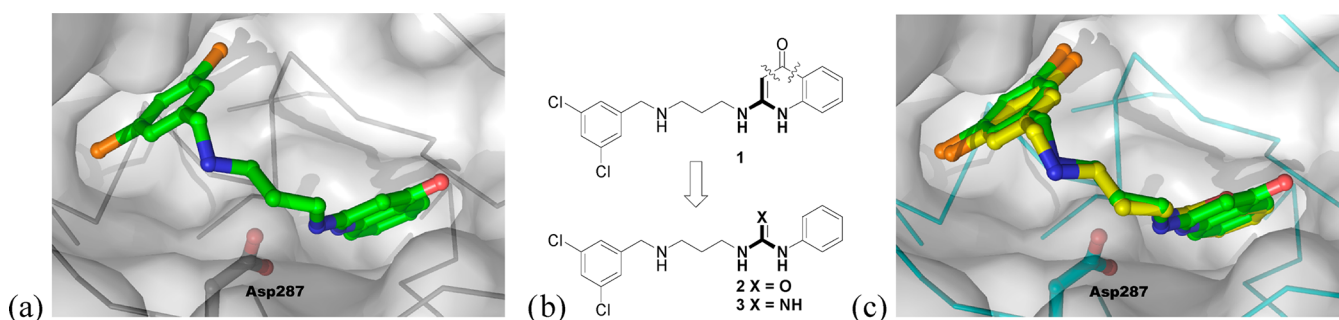
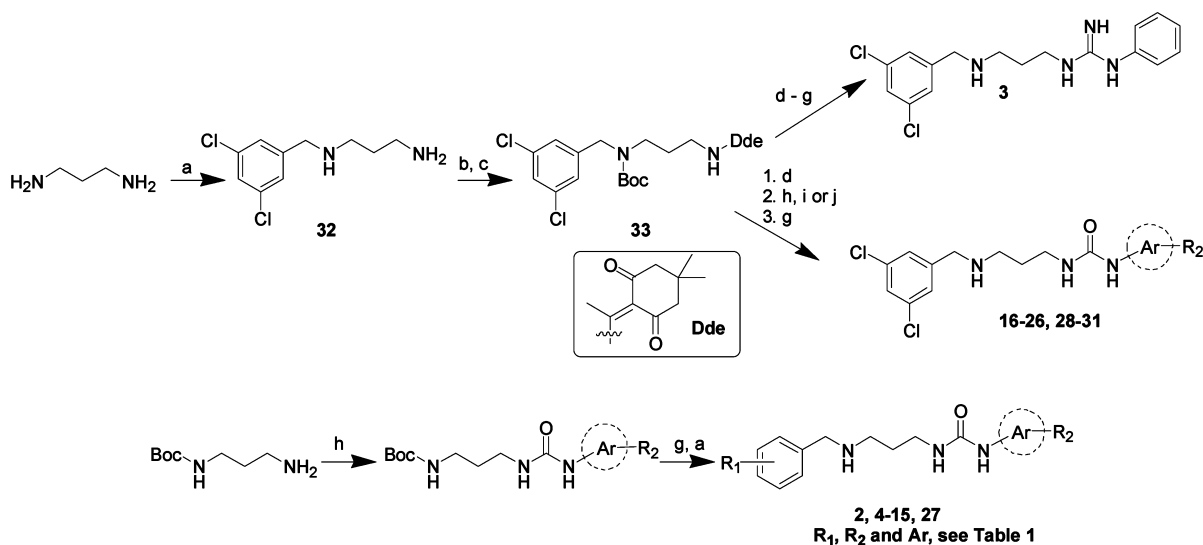


**Figure 1.** Docking study of aminoquinolone **1** and the design of urea and guanidine analogues using a *T. brucei* MetRS homology model.<sup>4</sup> (a) Docked pose of **1** with the two NHs of the aminoquinolone forming hydrogen bonds with Asp287; (b) design of urea **2** and guanidine **3**; (c) overlaid poses of **1** (carbons in green) and **2** (carbons in yellow) after docking.

### Scheme 1. Synthetic Routes<sup>a</sup>



<sup>a</sup>(a) Ar-CHO, AcOH, NaCNBH<sub>3</sub>, MeOH, rt; (b) 2-acetyldimmedone, DIPEA, CH<sub>2</sub>Cl<sub>2</sub>, MeOH, rt; (c) di-*tert*-butyl dicarbonate, K<sub>2</sub>CO<sub>3</sub>, MeCN, water, rt; (d) hydrazine, THF, microwave (65 °C, with 200 W maximum power input); (e) 1-isothiocyanatobenzene, CH<sub>2</sub>Cl<sub>2</sub>, rt; (f) HgCl<sub>2</sub>, 7 M NH<sub>3</sub> in MeOH; (g) TFA/CH<sub>2</sub>Cl<sub>2</sub> (1:4 v/v), rt; or H<sub>2</sub>O/TIPS/TFA (3:3:94, v/v), rt; (h) Ar-NCO, CH<sub>2</sub>Cl<sub>2</sub>, rt; (i) Ar-NH<sub>2</sub>, CDI, DMF, rt; (j) Ar-NH<sub>2</sub>, *p*-nitrophenyl chloroformate, DIPEA, THF, rt.

same position as the sulfur atom of methionine. The aminoquinolinone ring occupies an adjacent pocket, only created upon inhibitor binding, and forms hydrogen bonds through its NHs with the carboxylate of Asp 287 (Figure 1).

The Replidyne data and our docking study indicated the importance of a planar NH-X-NH in the aminoquinolone ring system for forming hydrogen bonds with the carboxylate of Asp287. This aspartate residue is strictly conserved in all MetRS enzymes based on a BLAST search that involved 250 sequence alignments and is responsible for substrate binding by forming a salt bridge to the  $\alpha$ -amino group of methionine.<sup>11</sup> Thus the aminoquinolone targets an enzyme active site amino acid residue that is unlikely to mutate, which is advantageous for drug discovery. However, the very same aminoquinolone moiety was suspected to be the potential cause of the inhibitor's poor bioavailability.<sup>5,6</sup> Therefore, we decided to move away from aminoquinolones but to keep a planar NH-X-NH moiety in our next generation of inhibitors. Conceptually dissecting the hetero ring system of the aminoquinolone led to a urea **2** or a guanidine **3** (Figure 1b). Literature search revealed that GlaxoSmithKline (GSK) has previously reported only one urea-based MetRS inhibitor for bacterial targets with moderate

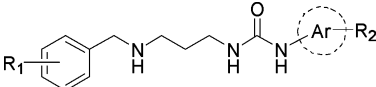
cellular activity.<sup>6</sup> In addition, Ibis Therapeutics reported a series of similar urea-based compounds for antibacterial chemotherapy with moderate activities although the compounds' target of action was not identified in their publication.<sup>12</sup> Therefore, urea or guanidine-based inhibitors against *T. brucei* MetRS warrant further systematic investigation using structure-based approaches. Molecular modeling demonstrated that the preferred binding conformations of urea or guanidine analogues superimposed nicely onto the aminoquinolone-based inhibitor (Figure 1c for urea **2**) and maintained the key hydrogen bond interactions with Asp287 as described before. As a result, compounds **2** and **3** were chosen as the initial testing candidates for synthesis, following Scheme 1.

For the aminoquinolone-based inhibitors, we previously reported an excellent correlation between *T. brucei* growth inhibition (EC<sub>50</sub>) and *T. brucei* MetRS thermal shift ( $\Delta T_m$ ),<sup>4</sup> a proxy for binding affinity where a 2 °C shift usually indicates significant binding.<sup>13–15</sup> By the same thermal shift assay, **2** and **3** exhibited  $\Delta T_m = 7.8 \pm 0.3$  °C and  $4.5 \pm 0.5$  °C, respectively, indicating that the urea-based **2** binds to the MetRS enzyme more tightly than the guanidine-based **3**. Hence, we selected

the urea-based **2** as the template in our exploration for inhibitors with good permeability properties.

**Affinity, Activity, and Selectivity of Urea-Based Inhibitors.** To explore the structure–activity–relationship (SAR), first the benzyl ring of **2** was modified by adding a hydrophobic substituent (–Cl, –OMe, and –OEt, see Scheme 1 and Table 1) to fill the mainly hydrophobic pocket. These

**Table 1.** Binding of Urea Compounds to *T. brucei* MetRS by a Thermal Shift Assay



compd	R <sub>1</sub>	aromatic ring	R <sub>2</sub>	<i>T. brucei</i> MetRS $\Delta T_m$ (°C) <sup>a</sup>
2	3,5-diCl	phenyl	H	7.8 ± 0.3
4	3-Cl,5-OMe	phenyl	H	7.7 ± 0.1
5	2,3,5-triCl	phenyl	H	6.4 ± 0.3
6	3-Cl	phenyl	H	5.5 ± 0.1
7	3-OMe	phenyl	H	4.7 ± 0.1
8	3-OEt	phenyl	H	2.7 ± 1.3
9	4-Cl	phenyl	H	2.5 ± 0.1
10	2-Cl	phenyl	H	1.9 ± 0.2
11	4-OMe	phenyl	H	1.1 ± 0.3
12	2-OEt	phenyl	H	1.1 ± 0.3
13	H	phenyl	H	1.3 ± 0.1
14	2-OMe	phenyl	H	1.1 ± 0.1
15	4-OEt	phenyl	H	0.5 ± 0.2
16	3,5-diCl	Phenyl	2-OH	8.4 ± 0.3
17	3,5-diCl	Phenyl	3-OH	7.7 ± 0.1
18	3,5-diCl	Phenyl	3-F	7.7 ± 0.1
19	3,5-diCl	phenyl	2-F	7.3 ± 0.1
20	3,5-diCl	Phenyl	4-F	6.3 ± 0.5
21	3,5-diCl	Phenyl	4-Cl	5.7 ± 0.2
22	3,5-diCl	Phenyl	3-Cl	5.2 ± 0.3
23	3,5-diCl	Phenyl	4-OH	5.8 ± 0.3
24	3,5-diCl	Phenyl	2-NH <sub>2</sub>	4.7 ± 0.2
25	3,5-diCl	phenyl	3-NH <sub>2</sub>	4.3 ± 0.2
26	3,5-diCl	3-thiophene	H	8.3 ± 0.9
27	3-Cl,5-OMe	3-thiophene	H	7.9 ± 0.1
28	3,5-diCl	2-thiophene	H	7.6 ± 0.3
29	3,5-diCl	3-pyridine	H	7.1 ± 0.1
30	3,5-diCl	2-pyridine	H	4.5 ± 0.2
31	3,5-diCl	4-pyridine	H	3.1 ± 0.1

<sup>a</sup> $\Delta T_m$  values are the average of three independent runs.

compounds were synthesized using the second route in Scheme 1 due to the need to vary the benzyl group on the left part of the molecule, which was attached last during synthesis. All three substitution positions (*ortho*-, *meta*-, and *para*-) exhibited a preference for the smaller substituents (–Cl, –OMe), with the *meta*- position exhibiting the highest  $\Delta T_m$  values among all other tested mono- and nonsubstituted compounds **6–15**.

Subsequently, the SAR around the aryl urea moiety was examined while keeping 3,5-dichlorobenzyl moiety on the other side of the molecule fixed (Scheme 1 and Table 1). Compounds were prepared using the first route shown in Scheme 1 so that the common part containing the 3,5-dichlorobenzyl moiety was synthesized first. As the aromatic ring of the aryl-urea is predicted to reside in a pocket that is created upon inhibitor binding, the pocket was anticipated to be somewhat flexible. Because the pocket consists of both

hydrophilic and hydrophobic residues, a variety of substituents (–OH, –NH<sub>2</sub>, –F, and –Cl) as well as heteroaromatic rings (thiophene and pyridine) were tested. From the  $\Delta T_m$  values, it can be seen that a hydroxyl group in *meta*- and *ortho*- positions is tolerated but that an amino group binds less favorably. Fluorine is preferred over chlorine. Substituted thiophene compounds **26–28** bind as well as the phenyl-based **2**. Among pyridine substituted compounds **29–31**, only the 3-pyridine **29** was nearly as active as **2**.

Choosing a minimum  $\Delta T_m$  threshold of 7.5 °C we selected a subset of compounds for confirmation of their inhibitory activity in an aminoacylation enzyme inhibition assay implemented for the *T. brucei* MetRS enzyme (Table 2). In this assay, the incorporation of <sup>3</sup>H-methionine into aminoacylated tRNA is measured. The IC<sub>50</sub>s ranged from 19 to 110 nM, thereby confirming the value of the  $\Delta T_m$  screen to find effective inhibitors, and **27** was the most potent.

We also examined these potent *T. brucei* MetRS inhibitors for selectivity. In the active site the sequence identity between *T. brucei* and human mitochondrial MetRS is 79%. With the human cytosolic enzyme, the identity in the active site is only 38%. Earlier, Replidyne scientists found that aminoquinolone inhibitors were 1000-fold better inhibitors of bacterial MetRS than the human mitochondrial enzyme and that they were virtually inactive against the human cytosolic enzyme.<sup>16</sup> Therefore, we tested our urea-based inhibitors only against human mitochondrial MetRS. As shown in Table 2, the tested compounds exhibited IC<sub>50</sub>s ranging from 4349 to >10000 nM, corresponding to a selectivity index of 39 or better.

The best urea-based inhibitors were tested in a *T. brucei brucei* growth inhibition assay (Table 2). The EC<sub>50</sub>s ranged from 150 to 757 nM, and **27** was most potent. An excellent linear correlation ( $R^2 = 0.95$ ) between *T. brucei* EC<sub>50</sub> and *T. brucei* MetRS IC<sub>50</sub> values was observed for the tested compounds, strongly supporting that these compounds inhibit *T. brucei* growth by targeting the MetRS enzyme (Figure 2).

To further establish that the MetRS inhibitors were acting “on target” in *T. brucei*, we performed experiments to demonstrate in vivo inhibition of protein synthesis. *T. brucei* cultures were incubated for 4 h (approximately 1 doubling time) with <sup>3</sup>H-histidine while in the presence of various test compounds. Newly synthesized protein was collected by precipitation with trichloroacetic acid and quantified by scintillation counting. Both the aminoquinolone MetRS inhibitor **1** and the urea compound **26** resulted in a dose-dependent decrease of incorporation of <sup>3</sup>H-amino acid into proteins similar to the protein synthesis inhibitor, cycloheximide (Figure 3). Two control compounds were also tested that act by mechanisms not directly related to protein synthesis: difluoromethylornithine (DFMO) that inhibits ornithine decarboxylase and subsequently polyamine biosynthesis, and a protein farnesyltransferase inhibitor (PFT inh) with anti-*T. brucei* activity.<sup>17</sup> Incubating *T. brucei* with these two compounds did not result in a dose-dependent decrease in protein synthesis (Figure 3). These results provide evidence that the MetRS inhibitors are blocking protein synthesis in cultured *T. brucei* as is expected by their mechanism of interfering with the normal processing of tRNA.

The compounds were also tested for host cell toxicity using a human lymphoblast cell line (CRL-8155) and a hepatocellular carcinoma cell line (Hep G2) (Table 2). These compounds showed toxicities to mammalian cell lines with EC<sub>50</sub>s ranging from 9.5 to 43  $\mu$ M, which translates into a selectivity index

Table 2. Enzymatic and Cellular Inhibitory Activity of Urea Compounds

compd	enzyme assays <sup>a</sup>			cell assays		
	<i>T. brucei</i> MetRS IC <sub>50</sub> (nM)	human mito MetRS IC <sub>50</sub> (nM)	selectivity index <sup>b</sup>		<i>T. brucei brucei</i>	
			human IC <sub>50</sub> / <i>T. brucei</i> IC <sub>50</sub>	EC <sub>50</sub> (nM)	CRL-8155 EC <sub>50</sub> (nM)	Hep G2 EC <sub>50</sub> (nM)
27	19	6591	347	150	22000	22000
17	29	5430	187	170	12000	12000
16	39	3720	95	210	>20000	>20000
26	28	4349	155	220	12000	13000
4	45	8348	186	330	20000	20000
2	57	>10000	>175	415	12000	20000
28	64	3056	48	350	9500	14500
18	110	4246	39	757	43200	17900

<sup>a</sup>Enzyme inhibition assay was measured in aminoacylation assays. <sup>b</sup>Selectivity Index: human mitochondrial MetRS IC<sub>50</sub> over *T. brucei* MetRS IC<sub>50</sub>.

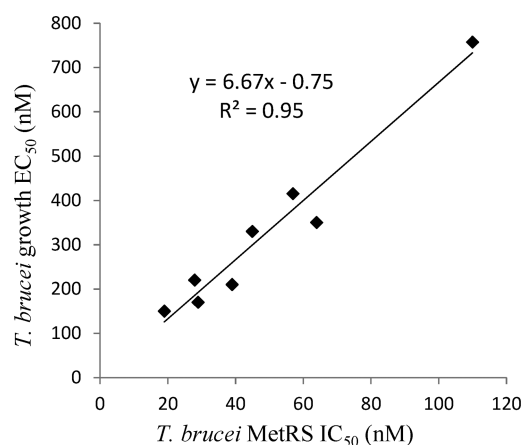


Figure 2. Correlation between enzyme (IC<sub>50</sub>) and parasite growth (EC<sub>50</sub>) inhibition for compounds listed in Table 2. Correlation coefficient R<sup>2</sup> is 0.95 ( $p < 0.0001$ ).

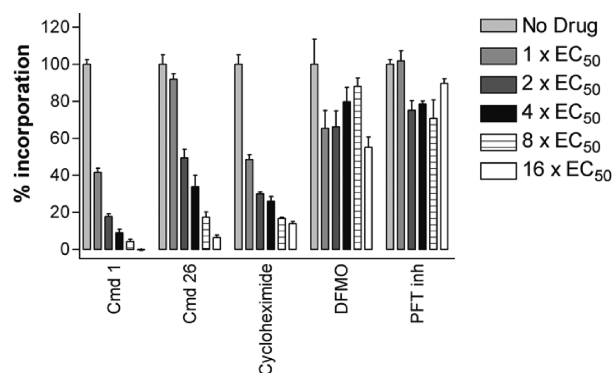


Figure 3. Protein synthesis inhibition in *T. brucei* cells. Midlog bloodstream form *T. brucei* were cultured with <sup>3</sup>H-histidine and various compounds at the indicated concentrations relating to their 48 h EC<sub>50</sub>. After 4 h, the cultures were harvested, proteins precipitated with trichloroacetic acid, and radiation quantified by scintillation counting.

between 27 and 147. Compound 27, which was the most potent *T. brucei* growth inhibitor with an EC<sub>50</sub> of 150 nM, showed the highest selectivity index of 147.

**Binding Mode to the Target MetRS.** Recently, we have obtained crystal structures of *T. brucei* MetRS in complex with six of the inhibitors discussed here. The binding of inhibitors to *T. brucei* MetRS resulted in large degree of structural changes in

the protein and will be the subject of another manuscript (Koh et al., manuscript under preparation). However, the binding mode of the inhibitors to the active site is in strong agreement with the model generated because the Replidyne poster had allowed us to incorporate conformational changes in the homology model. For example, superposition ( $\alpha$ -trace based) of the *T. brucei* MetRS:compound 2 crystal structure with the docking model of the same inhibitor revealed minimum differences in the binding site (Figure 4). Comparing the

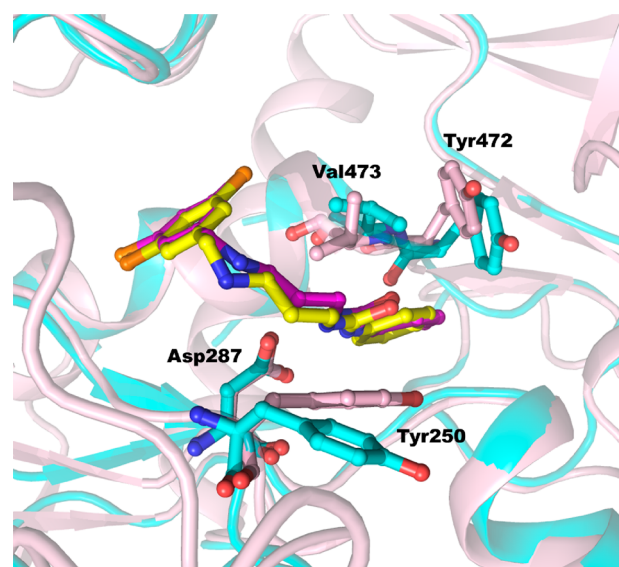


Figure 4. Superposition of *T. brucei* MetRS:2 complex (protein in pink) with the docking model of the same inhibitor (protein in cyan). The binding mode of 2 in the crystal structure (carbons in magenta) at the active site is in good agreement with that of the model (carbons in yellow).

two, the differences in atomic positions of the inhibitor are all less than 1 Å. The chlorine substituted benzyl ring binds to the methionine pocket, while the urea linked benzene forms a planar moiety that fits into the auxiliary pocket, as predicted by the model. The hydrophobic parts of Tyr250 and Tyr472–Val473 stack against the urea linked benzene, validating the importance of planarity in this part of the inhibitors. All other major interactions are otherwise similar. The hydrogen bonds between the urea NHs and Asp287, as well as the positioning of a *meta*-chlorine in the same site of the methionine sulfur atom, are all predicted correctly by the model. Therefore, the validity

of using the docking model to guide the design of new inhibitors is confirmed by the crystal structure.

**Membrane and Brain Permeability.** After we achieved high affinity binding to the target, potent activity against *T. brucei* cultures, and selectivity versus human model cells, it was particularly important to analyze the potential permeability of compounds to the CNS in order to develop drugs for treating late stage HAT. Hence, compounds **2**, **4**, **17**, **26**, and **27** were tested for permeability across a monolayer of MDRI-MDCKII cells that mimic the blood–brain barrier (Table 3).<sup>7–9</sup>

**Table 3.** Cell Permeability of Urea Compounds in the MDRI-MDCKII Model

compd	MDRI-MDCKII $P_{app}$ (nm/s)		AQ <sup>b</sup>
	–34 <sup>a</sup>	+34 <sup>a</sup>	
1	29 ± 8	52 ± 20	0.36 ± 0.33
2	356 ± 83	455 ± 62	0.21 ± 0.21
26	172 ± 55	317 ± 82	0.42 ± 0.28
27	97 ± 21	191 ± 3	0.53 ± 0.12
4	73 ± 9	150 ± 31	0.49 ± 0.16
17	29 ± 3	83 ± 31	0.62 ± 0.13

<sup>a</sup>Compound **34** is a P-gp pump inhibitor (see main text). <sup>b</sup>AQ: absorptive quotient.

Consistent with previous reports of poor oral absorption of the aminoquinolone compounds,<sup>6</sup> compound **1** was observed to have poor permeability through the MDRI-MDCKII monolayer (Table 3). Compounds that enter the central nervous system are typically associated with an apparent permeability  $P_{app} > 150$  nm/s.<sup>8</sup> This liability makes the aminoquinolone scaffold a poor candidate for HAT development because it is unlikely to be orally absorbed or pass through the blood–brain barrier. Two compounds in the urea series, **2** and **26**, exhibited a  $P_{app} > 300$  nm/s in the presence of P-gp inhibitor **34** (*N*-[4-[2-(6,7-dimethoxy-3,4-dihydro-1*H*-isoquinolin-2-yl)ethyl]phenyl]-5-methoxy-9-oxo-10*H*-acridine-4-carboxamide, GF120918),<sup>18</sup> indicating excellent intrinsic permeability of the compounds. Permeation of compounds **4**, **17**, and **27** were relatively low and were limited by P-gp efflux. Compound **26** exhibited a moderate  $P_{app}$  value of  $172 \pm 55$  nm/s measured in the absence of **34** compared to  $P_{app}$  value of  $317 \pm 82$  nm/s in the presence of **34**, with an absorptive quotient (AQ)<sup>9</sup> value of  $0.42 \pm 0.28$ , suggesting that compound **26** is a moderate substrate for P-gp. The permeability of compound **2** in the absence of **34** remained very high ( $P_{app}$ ,  $356 \pm 83$  nm/s), with an AQ value of  $0.21 \pm 0.21$ , indicating that P-gp efflux did not significantly limit the permeation of this compound.

To corroborate the in vitro permeability experiments, two compounds were tested for brain permeability in mice by a single dose of 5 mg/kg. As predicted from the in vitro model above, compound **1** demonstrated nearly undetectable brain levels at 60 min after IP injection. In contrast, compound **2** was actually concentrated in the brain ( $1.80 \pm 0.09 \mu\text{M}$ ) compared to plasma ( $0.12 \pm 0.02 \mu\text{M}$ ) (Figure 5). The mechanism of concentration remains to be characterized, but this feature is likely to be advantageous for treating second stage trypanosomiasis.

**Oral Bioavailability and in Vivo Efficacy of Urea-Based Inhibitors.** To further analyze the PK properties of the urea series, oral mouse PK experiments were performed with

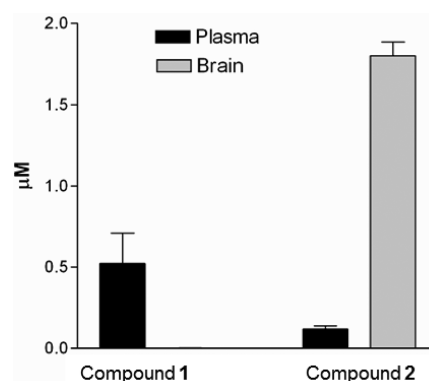
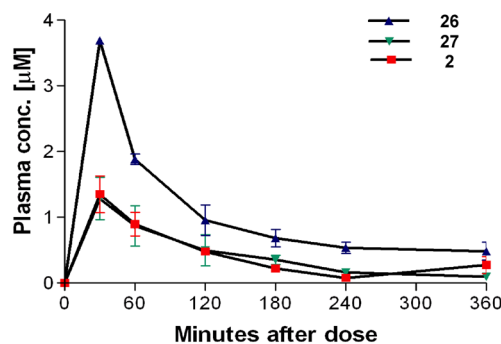


**Figure 5.** Concentrations of compounds **1** and **2** 60 min after IP injection in mice ( $n = 3$  per compound). The concentrations of **1** in the brain were at or below the limit of detection  $< 0.003 \mu\text{M}$ .

compounds **2**, **26**, and **27** (Figure 6). Compound **26** exhibited the best  $C_{max}$  at  $3.7 \pm 0.01 \mu\text{M}$  and a half-life of  $63 \pm 15$  min



Compound	$C_{max}$ ( $\mu\text{M}$ )	$T_{max}$ (min)	half-life (min)	AUC ( $\mu\text{M}\cdot\text{min}$ )
26	$3.7 \pm 0.01$	30	$63 \pm 15$	$464 \pm 69$
27	$1.29 \pm 0.57$	30	$82 \pm 15$	$161 \pm 84$
2	$1.35 \pm 0.49$	30	$65 \pm 27$	$152 \pm 59$

**Figure 6.** Pharmacokinetics characteristics of compounds **2**, **26**, and **27** in a mouse model. Mice ( $n = 3$  per group) were orally administered compounds by a single dose of 50 mg/kg.

with a moderate AUC level of  $464 \pm 69 \mu\text{M}\cdot\text{min}$  as an early lead compound. The overall mouse PK data suggested that the metabolic stability of compounds **2**, **26**, and **27** is reasonably good but may need further improvement by identifying and chemically modifying metabolically vulnerable fragments to further advance these aryl-urea moieties in the future. Regardless, the demonstrated oral bioavailability (Figure 6) and brain permeability (Figure 5) for the urea series of compounds are dramatic improvements of pharmacological properties over the aminoquinolone compounds.<sup>6</sup>

Next, we selected compound **26** to test in the murine model of acute *T. brucei* infection (Figure 7). This model uses the highly pathogenic *T. brucei rhodesiense* subspecies that causes rapidly rising parasitemia and death within about 4–5 days of infection. The mice were given **26** or vehicle starting 1 day after infection. At 48, 72, and 96 h postinfection, parasitemia was significantly reduced in the **26**-treated group compared to the vehicle-treated group by 94%, 80%, and 63%, respectively (Figure 7). Unfortunately, parasitemia continued to rise in the

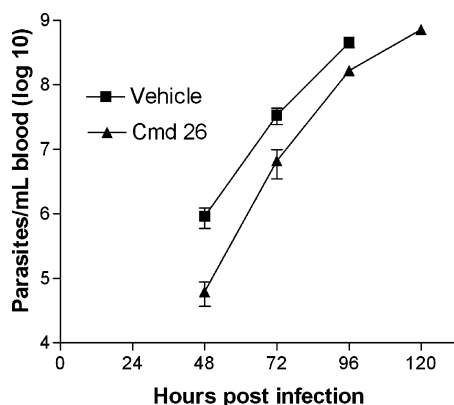


**Figure 7.** Suppression of *T. brucei* parasitemia in mice with **26**. Animals ( $n = 5$  per group) were infected with *T. brucei rhodesiense* at time 0, and treatment was initiated at 24 h postinfection. Mice received **26** or vehicle every 12 h for 4 days by oral administration. Mice were sacrificed when they became moribund (vehicle-treated mice were all sacrificed on day 4 and **26**-treated mice were sacrificed on day 5). Differences in parasitemia were significant at 48, 72, and 96 h ( $p = 0.030$ ,  $p = 0.027$ ,  $p = 0.008$ , respectively). The Y-axis is plotted on a log<sub>10</sub> scale.

**26** group and the animals needed to be euthanized when they became moribund at 120 h postinfection. No toxicity attributable to **26** was observed. Although there was a significant suppressive effect on parasitemia and an extension of survival for 1 day, the modest *in vivo* activity is easily explained by considering the pharmacodynamics of the experiment. First, when **26** was tested *in vitro* against the *rhodesiense* STIB900 strain, it has an EC<sub>50</sub> of 0.42  $\mu\text{M}$ . On the basis of the pharmacokinetic studies (Figure 4), the plasma concentrations of **26** are above the IC<sub>50</sub> for less than 6 h of the 12 hour dosing interval, and this is not considering the possibility that plasma protein binding may further reduce free compound levels in blood. In previous work, we found that *T. brucei* needed to be maintained with MetRS inhibitor at 8 times the EC<sub>50</sub> for 72 h to lead to irreversible killing *in vitro*.<sup>4</sup> On the basis of these considerations, it is actually satisfying to see a significant *in vivo* suppression of parasitemia with **26**. It is evident that more potent compounds (e.g., EC<sub>50</sub> of at least 0.05  $\mu\text{M}$  or less) with good pharmacokinetic profiles will be necessary to produce complete clearance of parasites in mice. With the aid of the recent crystal structure of urea compounds bound to the *T. brucei* MetRS, we hope to make progress in designing and synthesizing new compounds with the needed level of potency. For example, future plans to improve the potency of the urea inhibitors may involve making more extensive interactions with the methionyl substrate pocket as it appears that the current inhibitors do not fill up the entire volume of the pocket as confirmed by the crystal structure. Studies to address potential metabolic liabilities are also in progress, which may provide information on metabolism “hot-spots” that may be modified using structure-based design.

## CONCLUSIONS

In summary, we used the *T. brucei* MetRS homology model to guide rational modifications of the aminoquinolone scaffold and arrived at the new urea-based compounds that have improved PK properties. The homology model proved to be a high quality representation according to the X-ray structure of compound **2** bound to *T. brucei* MetRS. We were able to

achieve EC<sub>50</sub> values of 150 nM with a 147-fold selectivity over mammalian cell lines (compound **27**). Protein labeling studies provide evidence that the MetRS inhibitors block protein synthesis in *T. brucei* cells. Importantly, the new urea compounds (**2** and **26**) have high cell permeability according to MDR1-MDCKII cell assays and compound **2** demonstrated high levels of brain penetration in mice. Additionally, the urea compounds were observed to give good plasma levels in mice after oral dosing. Compound **26** led to significant suppression of *T. brucei rhodesiense* in mice but was not curative, probably due to its modest potency of  $\sim 0.4 \mu\text{M}$  against this strain. Through structure-based drug design, we hope to develop more potent compounds with the needed pharmacological properties to advance the urea series of MetRS inhibitors through preclinical development.

## EXPERIMENTAL METHODS

**Chemistry.** All starting materials were purchased from various chemical vendors and used without further purification unless noted. Silica was EMD 1.07734 Silica Gel 60 0.063–0.200 MM, 70–230 mesh ASTM, and TLC plates were Silica Gel IB-F. <sup>1</sup>H and <sup>13</sup>C NMR spectra were recorded on a Bruker AV-300 or AV-500. Chemical shifts ( $\delta$ ) are reported in parts per million (ppm) relative to internal CD<sub>3</sub>OD ( $\delta$  3.31 <sup>1</sup>H NMR,  $\delta$  49.2 <sup>13</sup>C NMR) or CDCl<sub>3</sub> ( $\delta$  7.24 <sup>1</sup>H NMR), the coupling constants ( $J$ ) are given in Hz. The abbreviations used are as follows: s, singlet; d, doublet; dd, double doublet; t, triplet; m, multiplet; p, pentet. ESI-MS were recorded on an Agilent 1100 LC/MSD Trap mass spectrometer. The purity of all final compounds **2–31** (>98%) was confirmed by reverse phase HPLC analysis monitored at 230 nm.

**1-(3-(3,5-Dichlorobenzylamino)propyl)-3-phenylurea (2).** To a solution of *tert*-butyl 3-aminopropylcarbamate (36  $\mu\text{L}$ , 0.21 mmol) in anhydrous CH<sub>2</sub>Cl<sub>2</sub> (1 mL) at 0 °C was added 1-isocyanatobenzene (25  $\mu\text{L}$ , 0.21 mmol). After the mixture was stirred overnight at room temperature, the solvent was removed *in vacuo*. Silica gel flash chromatography (30–60% EtOAc, hexane) yielded *tert*-butyl 3-(3-phenylureido)propylcarbamate (70 mg, quantitative) as a white solid. <sup>1</sup>H NMR (500 MHz, CDCl<sub>3</sub>)  $\delta$  7.13–7.39 (m, 5H), 7.01–7.09 (m, 1H), 5.73–5.81 (m, 1H), 5.02–5.10 (m, 1H), 3.23–3.31 (m, 2H), 3.15–3.21 (m, 2H), 1.56–1.66 (m, 2H), 1.46 (s, 9H). ESI-MS  $m/z$  294.1 (M + H)<sup>+</sup>.

To a solution of TFA:CH<sub>2</sub>Cl<sub>2</sub> (1:4) was added *tert*-butyl 3-(3-phenylureido)propylcarbamate (20 mg, 0.068 mmol). After the mixture was stirred for 3 h at room temperature, the solvent was removed *in vacuo*. The residues were redissolved in MeOH (10 mL). Sodium methoxide (4 mg, 0.07 mmol) was added to the mixture, and stirred for 15 min. Acetic acid (250  $\mu\text{L}$ ) and 3,5-dichlorobenzaldehyde (12 mg, 0.068 mmol) were added to the mixture, and stirred for 30 min, and then NaCNBH<sub>3</sub> (13 mg, 0.2 mmol) was added. After the mixture was stirred overnight at room temperature, the solvent was removed *in vacuo*. Silica gel flash chromatography (5% (10% NH<sub>4</sub>OH, 90% MeOH), CH<sub>2</sub>Cl<sub>2</sub>) yielded **2** (13 mg, 54%) as a white solid (mp 96–97 °C). <sup>1</sup>H NMR (500 MHz, MeOD)  $\delta$  7.32–7.45 (m, 5H), 7.26 (t,  $J = 7.9$  Hz, 2H), 7.00 (t,  $J = 7.3$  Hz, 1H), 3.76 (s, 2H), 3.27 (t,  $J = 6.7$  Hz, 2H), 2.66 (t,  $J = 7.1$  Hz, 2H), 1.66–1.83 (m, 2H). <sup>13</sup>C NMR (126 MHz, MeOD)  $\delta$  157.08, 143.58, 139.55, 134.67, 128.39, 126.75, 126.64, 122.04, 118.89, 52.01, 45.80, 37.18, 29.61. ESI-MS  $m/z$  353.3 (M + H)<sup>+</sup>.

**N<sup>1</sup>-(3,5-Dichlorobenzyl)propane-1,3-diamine (32).** 3,5-Dichlorobenzaldehyde (100 mg, 0.57 mmol) was added to a solution of propyldiamine (500  $\mu\text{L}$ , 6 mmol) and AcOH (3 mL) in MeOH (10 mL). After the mixture was stirred for 30 min, NaCNBH<sub>3</sub> (50 mg, 0.79 mmol) was added. The mixture was stirred overnight and the solvent was removed *in vacuo*. The residues were washed with EtOAc and 1 M NaOH (aq). The organic layer was dried over MgSO<sub>4</sub> and concentrated *in vacuo*, yielding the desired product **32** (120 mg, 90%) as a colorless oil. ESI-MS  $m/z$  234.1 (M + H)<sup>+</sup>. <sup>1</sup>H NMR (300

MHz, CDCl<sub>3</sub>)  $\delta$  7.25–7.15 (m, 3H), 3.74 (s, 2H), 2.80 (t,  $J$  = 6.9 Hz, 2H), 2.68 (t,  $J$  = 6.9 Hz, 2H), 1.66 (p,  $J$  = 7.5 Hz, 2H).

**tert-Butyl 3,5-dichlorobenzyl(3-(1-(4,4-dimethyl-2,6-dioxocyclohexylidene)ethyl-amino)propyl)carbamate (33).** 2-Acetyldimedone (Dde-OH) (70 mg, 0.39 mmol) was added to a solution of **32** (90 mg, 0.39 mmol) and DIPEA (0.13 mL, 0.77 mmol) in MeOH (0.5 mL) and CH<sub>2</sub>Cl<sub>2</sub> (10 mL). After the mixture was stirred overnight at room temperature, the solvent was removed in vacuo. Silica gel flash chromatography (4% MeOH, CH<sub>2</sub>Cl<sub>2</sub>) afforded the desired intermediate. Di-*tert*-butyl dicarbonate (72 mg, 0.33 mmol) was added to a solution of the intermediate (130 mg, 0.33 mmol) and K<sub>2</sub>CO<sub>3</sub> (45 mg, 0.33 mmol) in 10% water and 90% MeCN (15 mL). After the reaction mixture was stirred overnight at room temperature, the solvent was removed in vacuo. The residues were washed with EtOAc and brine. The organic layer was dried over anhydrous MgSO<sub>4</sub>, filtered, and then concentrated in vacuo. Silica gel flash chromatography (10–50% EtOAc, hexane) afforded the corresponding product **33** (100 mg) as a colorless oil. <sup>1</sup>H NMR (500 MHz, MeOD)  $\delta$  7.34 (s, 1H), 7.24 (s, 2H), 4.44 (s, 2H), 3.46–3.53 (m, 2H), 3.34–3.44 (m, 2H), 2.53 (s, 3H), 2.37 (s, 4H), 1.88–1.96 (m, 2H), 1.47 (s, 9H), 1.03 (s, 6H). ESI-MS  $m/z$  498.1 (M + H)<sup>+</sup>.

**1-[3-(3,5-Dichloro-benzylamino)-propyl]-3-thiophen-3-yl-urea (26).** Anhydrous hydrazine (6.7  $\mu$ L, 0.20 mmol) was added to a solution of **33** (35 mg, 0.071 mmol) in anhydrous THF (1 mL). The mixture was irradiated with microwave (a CEM Discover system, 200 W maximum input power) to maintain at 65 °C for 30 min. The solvent was removed in vacuo, and the residue was redissolved in anhydrous CH<sub>2</sub>Cl<sub>2</sub> (0.5 mL). To the mixture at 0 °C was added 3-isocyanatothiophene (9 mg, 0.071 mmol), and the mixture was stirred overnight at room temperature. The solvent was removed in vacuo, and the residues were purified by silica gel flash chromatography (EtOAc, hexane). The purified intermediate was added to a solution of 3% H<sub>2</sub>O, 3% TIPS, and 94% TFA (1 mL). The solvent was removed in vacuo, and silica gel flash chromatography (8% (10% NH<sub>4</sub>OH, 90% MeOH), CH<sub>2</sub>Cl<sub>2</sub>) yielded the desired product **26** (20 mg, 79%) as a white solid (mp 103–104 °C). <sup>1</sup>H NMR (500 MHz, MeOD)  $\delta$  7.31–7.40 (m, 3H), 7.27 (dd,  $J$  = 3.2, 5.2 Hz, 1H), 7.14 (dd,  $J$  = 1.4, 3.2 Hz, 1H), 6.94 (dd,  $J$  = 1.4, 5.2 Hz, 1H), 3.77 (s, 2H), 3.27 (t,  $J$  = 6.6 Hz, 2H), 2.66 (t,  $J$  = 7.1 Hz, 2H), 1.70–1.79 (m, 2H). <sup>13</sup>C NMR (126 MHz, MeOD)  $\delta$  156.96, 143.17, 137.28, 134.69, 126.81, 126.75, 123.69, 121.06, 106.40, 51.91, 45.73, 37.22, 29.49. ESI-MS  $m/z$  359.2 (M + H)<sup>+</sup>.

**1-[3-(3-Chloro-5-methoxy-benzylamino)-propyl]-3-thiophen-3-yl-urea (27).** 3-Isocyanatothiophene (36 mg, 0.29 mol) was added to a solution of *tert*-butyl 3-aminopropylcarbamate (50 mg, 0.29 mmol) in anhydrous CH<sub>2</sub>Cl<sub>2</sub> at 0 °C. After the reaction was stirred overnight at room temperature, the solvent was removed in vacuo. Silica gel flash chromatography (30–60% EtOAc, hexane) afforded *tert*-butyl 3-(3-(thiophen-3-yl)ureido)propylcarbamate (60 mg, 70%). To a solution 3% H<sub>2</sub>O, 3% TIPS, and 94% TFA (1 mL) was added *tert*-butyl 3-(3-(thiophen-3-yl)ureido)propylcarbamate (28 mg, 0.094 mol). After the mixture was stirred for 1 h at room temperature, the solvent was removed in vacuo. Residues were redissolved in MeOH (10 mL). Sodium methoxide (5 mg, 0.094 mol) was added to the mixture and stirred for 15 min. Acetic acid (250  $\mu$ L) and 3-chloro-5-methoxybenzaldehyde (16 mg, 0.094 mol) were added to the mixture, stirred for 30 min, and then NaCNBH<sub>3</sub> (9 mg, 0.14 mmol) was added to the mixture. After the mixture was stirred overnight, the solvent was removed in vacuo. Silica gel flash chromatography (9% (10% NH<sub>4</sub>OH, 90% MeOH), CH<sub>2</sub>Cl<sub>2</sub>) yielded the desired product **27** (15 mg, 45%) as a colorless oil. <sup>1</sup>H NMR (500 MHz, MeOD)  $\delta$  7.28 (ddd,  $J$  = 1.8, 3.2, 5.1 Hz, 1H), 7.16 (dd,  $J$  = 1.4, 3.2 Hz, 1H), 7.03 (q,  $J$  = 1.6 Hz, 1H), 6.97 (dd,  $J$  = 1.4, 5.1 Hz, 1H), 6.94 (q,  $J$  = 1.8 Hz, 1H), 6.91 (q,  $J$  = 2.0 Hz, 1H), 3.85 (s, 2H), 3.82 (s, 3H), 3.29 (t,  $J$  = 6.6 Hz, 2H), 2.78 (t,  $J$  = 7.1 Hz, 2H), 1.81 (p,  $J$  = 5.7, 6.6 Hz, 2H). <sup>13</sup>C NMR (126 MHz, MeOD)  $\delta$  160.78, 157.14, 140.34, 137.23, 134.65, 123.72, 121.07, 120.64, 113.19, 112.75, 106.47, 54.70, 52.00, 45.46, 36.93, 28.92. ESI-MS  $m/z$  354.9 (M + H)<sup>+</sup>.

**Protein Expression and Purification.** Full-length *T. brucei* MetRS was expressed and purified as previously described<sup>4</sup> and used throughout the study except for crystallization experiments. Human mitochondrial MetRS was expressed as reported<sup>19</sup> with plasmid provided by Dr. Spemulli.

**Protein Crystallization and Structure Determination.** Detailed descriptions of protein crystallization and structure determination will be reported in a separate manuscript (Koh et al., manuscript under preparation). The structure of the complex of *T. brucei* MetRS and **2** was deposited to the Protein Data Bank (PDB ID code: 3TUN).

**Thermal Shift Assay.** The thermal shift assay was performed as previously described<sup>4,15</sup> with the modifications that samples contained the MetRS enzyme (0.4 mg/mL for *T. brucei* enzyme), 100  $\mu$ M of inhibitor, and 5% DMSO. The assays were repeated three times independently.

***T. brucei* Methionyl-tRNA Synthetase Aminoacylation Assay.** Enzyme activity was quantified by the attachment of [<sup>3</sup>H]methionine to tRNA in the presence of the *T. brucei* MetRS enzyme. Reactions were performed in 96-well filter plates with Durapore membranes (MSHVN4B10; Millipore) in volumes of 75  $\mu$ L. The reaction was performed with 25 mM HEPES (pH 7.9), 10 mM MgCl<sub>2</sub>, 50 mM KCl, 0.2 mM spermine, 0.1 mg/mL bovine serum albumin, 2.5 mM dithiothreitol, 1% DMSO, and 1 U/mL pyrophosphatase (I1643; Sigma). Recombinant enzyme (10 nM) and compound inhibitors (starting concentration varied depending on potency and included 12 serial two dilutions) were mixed with the buffer and preincubated for 15 min. To start the reaction, 400  $\mu$ g/mL bulk *Escherichia coli* tRNA (R4251; Sigma), 0.1 mM ATP, and 250 nM [<sup>3</sup>H]methionine (80 Ci/mmol) were added. The plate was incubated without shaking at room temperature for 120 min. The reactions were stopped by the addition of 100  $\mu$ L of cold 10% trichloroacetic acid. The reaction components were separated from tRNA by filtration through a vacuum manifold and washed three times with cold 10% trichloroacetic acid. The filter plates were dried overnight, scintillation fluid was added, and the counts on the plates were determined in a scintillation plate counter. Samples were run in quadruplicate, and percent inhibition was calculated using two different controls (no enzyme and no test compound) with the following formula:

$$\% \text{inhibition} = 100 \times (\text{Mnd} - \text{Dtd}) / (\text{Mnd} - \text{Mne})$$

where Mnd is the average no drug control, Dtd is each test drug value, and Mne is the average no enzyme control. IC<sub>50</sub> values were then calculated by nonlinear regression (sigmoidal dose response) in Prism 3.0.

**Human Mitochondrial Methionyl-tRNA Synthetase Aminoacylation Assay.** Assays were performed as described above except for the following changes. Enzyme activity was quantified by the attachment of [<sup>3</sup>H]methionine to tRNA in the presence of the human mitochondrial MetRS enzyme. The reaction was performed with 50 mM Tris-HCl (pH 8.0), 2.5 mM MgCl<sub>2</sub>, 2.5 mM KCl, 0.2 mM spermine, 0.2 mg/mL bovine serum albumin, 2.5 mM dithiothreitol, and 1 U/mL pyrophosphatase (I1643; Sigma). Recombinant enzyme (20 nM) and compound inhibitors (starting concentration varied depending on potency and included 12 serial two dilutions) were mixed with the buffer and preincubated for 15 min. To start the reaction, 200  $\mu$ g/mL bulk *E. coli* tRNA (R4251; Sigma), 2.5 mM ATP, and 250 nM [<sup>3</sup>H]methionine (80 Ci/mmol) were added. The plate was incubated without shaking at 37 °C for 120 min.

***T. brucei* Growth Inhibition Assay.** *T. brucei brucei* (bloodstream form strain 427 from K. Stuart, Seattle BioMed, Seattle, WA) were cultured in HMI-9 medium containing 10% fetal bovine serum, penicillin, and streptomycin at 37 °C with 5% CO<sub>2</sub> and *T. brucei rhodesiense* (bloodstream form STIB900 from Simon Croft, London School of Hygiene and Tropical Medicine, UK) were grown in HMI-18 containing 20% fetal bovine serum, penicillin, and streptomycin.<sup>20</sup> Drug sensitivity of the *T. brucei* strain was determined in 96-well microtiter plates in triplicate with an initial inoculum of 5  $\times$  10<sup>4</sup> trypanomastigotes per well. Compound stock solutions were prepared in DMSO at 20 mM and added in serial dilutions for a final volume of

200  $\mu\text{L}$ /well. Parasite growth was quantified at 48 h by the addition of Alamar Blue (Alamar Biosciences, Sacramento, CA).<sup>21</sup> Pentamidine isethionate (Sigma-Aldrich) was included in each assay as a positive control. Standard errors within assays were consistently less than 15%.

**Protein Synthesis Inhibition Assay.** Midlog phase *T. brucei* cells ( $5 \times 10^5$ ) were added to wells of a 96-well plate in a 100  $\mu\text{L}$  volume of HMI-9 media. Compounds at concentrations ranging from 1 to 16 times the 48 h  $\text{EC}_{50}$  were added to the plated cells in triplicate and allowed to incubate for 15 min, with a no-drug control included for each plate. [<sup>3</sup>H]-L-histidine (1 mCi/ml, 47.9 Ci/mmol) (Moravak Biochemicals, Brea, CA) in a volume of 20  $\mu\text{L}$  of PBS was added to each well and incubated with the parasites for 4 h. Cycloheximide and difluoromethylornithine were purchased from Sigma-Aldrich; the PFT inhibitor corresponds to compound 4g in a previous publication.<sup>17</sup> The experiment was stopped by adding 100  $\mu\text{L}$  of 20% trichloroacetic acid and placed at 4 °C for 15 min. Plates were harvested onto a PerkinElmer Unifilter-96 GF/B filter using an Inotech Biosystems cell harvester and washed twice with 5% trichloroacetic acid. The filters were dried overnight in a vacuum oven and then finished by raising the temperature to 40 °C for 3 h. Scintillation fluid was added, and the filters were counted using a PerkinElmer MicroBeta2 scintillation counter. These methods were adapted from Rock et al.<sup>22</sup>

**Mammalian Cell Growth Inhibition Assays.** The human lymphocytic cell line CRL-1855 (American Type Culture Collection) were grown in RPMI medium (Lonza, Walkersville, MD) with 10% fetal bovine serum at 37 °C with 5%  $\text{CO}_2$ . The human hepatocellular cell line HepG2 (American Type Culture Collection) were grown in DMEM/F-12 medium (Lonza, Walkersville, MD) with 10% fetal calf serum. Cells ( $5 \times 10^3$ /well) were added to 96-well plates and incubated with serial dilutions of compounds for 48 h. At that time, cell viability was quantified by addition of Alamar Blue, and plates were incubated for an additional 4 h at 5%  $\text{CO}_2$ , 37 °C. Absorbance readings ( $\text{OD}_{570-600}$ ) were used to calculate viability referenced against cells grown with no inhibitors.

**MDR1-MDCKII Assay.** Compounds and the controls, Amprenavir (Moravak Biochemicals) and Propranolol (Sigma), were tested in triplicate at a final concentration of 3  $\mu\text{M}$  with and without 2  $\mu\text{M}$  34 (Elacridar, Toronto Research Chemicals Inc.). Amprenavir gives moderate–high permeability without 34 (typically  $P_{\text{app}} > 200$ ) but is reversed by 34 (AQ > 0.5), whereas Propranolol gives high permeability without reversal with 34 (typically  $P_{\text{app}} > 300$  and AQ < 0.5). MDR1-MDCKII cells were cultured at 37 °C in 5%  $\text{CO}_2$  in cell culture media containing 500 mL of Dulbecco's Modified Eagle's Medium with GlutaMAX (GIBCO) supplemented with 50 mL of fetal bovine serum (GIBCO) and 5 mL of penicillin–streptomycin (Sigma). Then  $3.3 \times 10^5$  MDR1-MDCKII cells were plated in the hanging insert (apical chamber) of the 12-well Transwell plates (Corning-Costar) in 0.5 mL of cell culture media. An additional 1.5 mL of cell culture media was added to the bottom (basolateral) chamber. The assay was conducted three days later at 37 °C in 5%  $\text{CO}_2$  in transport media containing 500 mL of Hank's Balanced Salt Solution (Sigma) supplemented with 12.5 mL of 1 M glucose (Sigma) and 12.5 mL of 1 M HEPES buffer (Sigma).

On the day of the assay, the cell culture media was replaced with transport media with and without 2  $\mu\text{M}$  34 and preincubated for approximately 30 min. Transepithelial electrical resistance (TEER) values were then recorded using the Millicell-ERS (Millipore). The transport media was then aspirated, and compounds and controls were added to the inserts at a final concentration of 3  $\mu\text{M}$  in 0.4 mL of transport media with and without 2  $\mu\text{M}$  34. Plates were incubated with shaking (~60 rpm) for 60 min. Immediately following incubation, two 100  $\mu\text{L}$  aliquots were taken from both chambers and the amount of drug was measured by mass spectroscopy. Lucifer Yellow (Aldrich), a fluorescence compound used to test membrane integrity during the assay, was then added to the inserts at a final concentration of 250  $\mu\text{M}$  and incubated for 60 min with shaking (~60 rpm). After this final incubation, 100  $\mu\text{L}$  aliquots were transferred to a black 96-well plate (BD Falcon) and fluorescence was measured for each membrane, and TEER values were again recorded. Mass spectroscopy analysis was performed on samples with Lucifer Yellow  $P_{\text{app}}(A - B)$  values < 20

nm/s and TEER values > 200 ohm/cm<sup>2</sup>. The  $P_{\text{app}}(A - B)$  or apparent permeability coefficient for each compound was calculated and reported in nm/s.

$$P_{\text{app}} = (dQ/dt)/(A \times C_0)$$

where dQ is the amount of compound that has crossed the membrane, dt is the incubation time of the assay, A is the area of the cell monolayer, and  $C_0$  is the initial concentration in the donor well.

The absorptive quotient (AQ) previously described by Troutman and Thakker<sup>9</sup> identifies compounds that may be P-gp pump substrates by quantifying the functional activity of the P-gp pump during absorptive transport. An AQ value  $\geq 0.5$  is associated with high affinity for the P-gp pump.

**Measurement of Brain Permeability in Mice.** All studies described in this paper using mice were done under an approved IACUC protocol at University of Washington. Six–eight week old Swiss Webster female mice (CFW, Charles River, Wilmington, MA) were administered compound 1 or 2 by IP injection with a dose of 5 mg/kg. The compounds were dissolved in a solution of 5% DMSO, 3% EtOH, and 7% Tween 80 in saline. Each compound was administered to three mice, and at 1 h they were sacrificed by cervical dislocation, blood was collected in heparinized capillary tubes, and brains removed and frozen at –80 °C. Plasma was separated from whole blood and frozen for later analysis. Ten  $\mu\text{L}$  of plasma were extracted with 30  $\mu\text{L}$  of acetonitrile containing an extraction standard. Thawed brain tissue was homogenized in PBS containing an extraction standard using a Pyrex tissue grinder and then extracted with 4 mL of acetonitrile. Blank mouse brains spiked with known amount of compound were used to standardize the assay. The samples were centrifuged and the supernatants dried under vacuum. Samples were dissolved again in acetonitrile, and compound concentrations were quantified on a Waters Quattro Micro in MS/MS mode attached to an Agilent HPLC system as described.<sup>23</sup>

**Pharmacokinetic Studies in Mice.** Pharmacokinetic studies of compounds 2, 26, and 27 were performed by orally administering to mice 50 mg/kg of compounds dissolved in 5% DMSO, 3% EtOH, and 7% Tween 80 in saline solution. Three mice were used per group. Then 40  $\mu\text{L}$  of blood was collected at time points of 0.5, 1, 2, 3, 4, and 6 h post injection via tail snips. The plasma samples were extracted with acetonitrile and analyzed as described above.<sup>23</sup>

**Efficacy Studies in Mice.** Five female 6–8 week old Swiss Webster (CFW) mice (Charles River, Wilmington, MA) were used per group. At time 0, each mouse was infected by IP injection with  $1 \times 10^4$  bloodstream forms of *T. rhodesiense* STIB900 (gift of Simon Croft, London School of Hygiene and Tropical Medicine, UK) in 0.2 mL. Treatment with compounds was initiated at 24 h postinfection. Compound 26 was mixed in vehicle of 5% DMSO, 3% EtOH, and 7% Tween 80 in saline solution and administered at a dose of 50 mg/kg every 12 h for 4 days by oral gavage (0.2 mL per mouse). A second group received vehicle alone every 12 h for 4 days (0.2 mL) by oral gavage. Parasitemia was monitored daily by microscopic examination of tail blood on wet mounts. Statistical analysis on individual days was performed by unpaired *t* tests.

## ■ ASSOCIATED CONTENT

### 📄 Supporting Information

Additional synthesis and compound characterization details. This material is available free of charge via the Internet at <http://pubs.acs.org>.

### Accession Codes

PDB ID code 3TUN.

## ■ AUTHOR INFORMATION

### Corresponding Author

\* For F.B.: phone, (206) 616-9214; fax, (206) 685-6045; E-mail, [fbuckner@uw.edu](mailto:fbuckner@uw.edu); address, University of Washington, Division of Allergy and Infectious Diseases, Box 357185,



Seattle, WA 98195. For E.F.: phone, (206) 685-7048; fax, (206)-685-7002; E-mail: erkang@uw.edu; address, University of Washington, Department of Biochemistry and Biomolecular Structure Center, Box 357742, Seattle, WA 98195.

### Notes

The authors declare no competing financial interest.

### ACKNOWLEDGMENTS

Support for this research was provided by the National Institutes of Health grants AI067921 and AI084004. We are grateful to Colin McMartin and Regine Bohacek for providing the FLO/QXP software, Robert Jacobs and Cindy Rewerts from Scynexis for advice and assistance in MDR1-MDCKII assay, Zhongsheng Zhang and Baoshun Zhang for technical assistance, Sharon Creason for performing mammalian cell cytotoxicity assays, Matthew Hulverson for assisting with pharmacokinetic experiments, Linda Spremulli for providing expression plasmid of human MetRS, and Wesley Van Voorhis, Alberto Napuli, and the protein production unit of the Medical Structural Genomics of Pathogenic Protozoa (MSGPP) program for protein expression.

### ABBREVIATIONS USED

HAT, human African trypanosomiasis; MetRS, methionyl-tRNA synthetase; aaRS, aminoacyl-tRNA synthetase; MDCK, Madin–Darby canine kidney; BLAST, Basic Local Alignment Search Tool; AQ, absorptive quotient

### REFERENCES

- (1) Rodgers, J. Human African trypanosomiasis, chemotherapy and CNS disease. *J. Neuroimmunol.* **2009**, *211*, 16–22.
- (2) Brun, R.; Blum, J.; Chappuis, F.; Burri, C. Human African trypanosomiasis. *Lancet* **2010**, *375*, 148–159.
- (3) Sheppard, K.; Yuan, J.; Hohn, M. J.; Jester, B.; Devine, K. M.; Soll, D. From one amino acid to another: tRNA-dependent amino acid biosynthesis. *Nucleic Acids Res.* **2008**, *36*, 1813–1825.
- (4) Shibata, S.; Gillespie, J. R.; Kelley, A. M.; Napuli, A. J.; Zhang, Z.; Kovzun, K. V.; Pefley, R. M.; Lam, J.; Zucker, F. H.; Van Voorhis, W. C.; Merritt, E. A.; Hol, W. G.; Verlinde, C. L.; Fan, E.; Buckner, F. S. Selective inhibitors of methionyl-tRNA synthetase have potent activity against *Trypanosoma brucei* infection in Mice. *Antimicrob. Agents Chemother.* **2011**, *55*, 1982–1989.
- (5) Jarvest, R. L.; Berge, J. M.; Berry, V.; Boyd, H. F.; Brown, M. J.; Elder, J. S.; Forrest, A. K.; Fosberry, A. P.; Gentry, D. R.; Hibbs, M. J.; Jaworski, D. D.; O'Hanlon, P. J.; Pope, A. J.; Rittenhouse, S.; Sheppard, R. J.; Slater-Radosti, C.; Worby, A. Nanomolar inhibitors of *Staphylococcus aureus* methionyl tRNA synthetase with potent antibacterial activity against gram-positive pathogens. *J. Med. Chem.* **2002**, *45*, 1959–1962.
- (6) Jarvest, R. L.; Armstrong, S. A.; Berge, J. M.; Brown, P.; Elder, J. S.; Brown, M. J.; Copley, R. C. B.; Forrest, A. K.; Hamprecht, D. W.; O'Hanlon, P. J.; Mitchell, D. J.; Rittenhouse, S.; Witty, D. R. Definition of the heterocyclic pharmacophore of bacterial methionyl tRNA synthetase inhibitors: potent antibacterially active non-quinolone analogues. *Bioorg. Med. Chem. Lett.* **2004**, *14*, 3937–3941.
- (7) Wang, Q.; Rager, J. D.; Weinstein, K.; Kardos, P. S.; Dobson, G. L.; Li, J.; Hidalgo, I. J. Evaluation of the MDR-MDCK cell line as a permeability screen for the blood–brain barrier. *Int. J. Pharm.* **2005**, *288*, 349–359.
- (8) Mahar Doan, K. M.; Humphreys, J. E.; Webster, L. O.; Wring, S. A.; Shampine, L. J.; Serabjit-Singh, C. J.; Adkison, K. K.; Polli, J. W. Passive Permeability and P-Glycoprotein-Mediated Efflux Differentiate Central Nervous System (CNS) and Non-CNS Marketed Drugs. *J. Pharmacol. Exp. Ther.* **2002**, *303*, 1029–1037.
- (9) Troutman, M. D.; Thakker, D. R. Novel experimental parameters to quantify the modulation of absorptive and secretory transport of

compounds by P-glycoprotein in cell culture models of intestinal epithelium. *Pharm. Res.* **2003**, *20*, 1210–1224.

- (10) Evans, R.; Green, L.; Sun, X.; Guiles, J.; Lorimer, D.; Burgin, A.; Janjic, N.; Jarvis, T.; Davies, D. Co-crystal structure of REP3123 bound to *Clostridium difficile* methionyl tRNA synthetase, poster F1–2114. In *Abstracts of the 47th International Conference on Antimicrobial Agents and Chemotherapy*; American Society for Microbiology: Washington, DC, 2007.

- (11) Larson, E. T.; Kim, J. E.; Zucker, F. H.; Kelley, A.; Mueller, N.; Napuli, A. J.; Verlinde, C. L. M. J.; Fan, E.; Buckner, F. S.; Van Voorhis, W. C.; Merritt, E. A.; Hol, W. G. J. Structure of *Leishmania major* methionyl-tRNA synthetase in complex with intermediate products methionyladenylate and pyrophosphate. *Biochimie* **2011**, *93*, 570–582.

- (12) Seth, P. P.; Ranken, R.; Robinson, D. E.; Osgood, S. A.; Risen, L. A.; Rodgers, E. L.; Migawa, M. T.; Jefferson, E. A.; Swayze, E. E. Aryl urea analogs with broad-spectrum antibacterial activity. *Bioorg. Med. Chem. Lett.* **2004**, *14*, 5569–5572.

- (13) Pantoliano, M. W.; Petrella, E. C.; Kwasnoski, J. D.; Lobanov, V. S.; Myslik, J.; Graf, E.; Carver, T.; Asel, E.; Springer, B. A.; Lane, P.; Salemme, F. R. High-density miniaturized thermal shift assays as a general strategy for drug discovery. *J. Biomol. Screening* **2001**, *6*, 429–440.

- (14) Lo, M. C.; Aulabaugh, A.; Jin, G. X.; Cowling, R.; Bard, J.; Malamas, M.; Ellestad, G. Evaluation of fluorescence-based thermal shift assays for hit identification in drug discovery. *Anal. Biochem.* **2004**, *332*, 153–159.

- (15) Crowther, G. J.; Napuli, A. J.; Thomas, A. P.; Chung, D. J.; Kovzun, K. V.; Leibly, D. J.; Castaneda, L. J.; Bhandari, J.; Damman, C. J.; Hui, R.; Hol, W. G.; Buckner, F. S.; Verlinde, C. L.; Zhang, Z.; Fan, E.; Van Voorhis, W. C. Buffer optimization of thermal melt assays of Plasmodium proteins for detection of small-molecule ligands. *J. Biomol. Screening* **2009**, *14*, 700–707.

- (16) Green, L. S.; Bullard, J. M.; Ribble, W.; Dean, F.; Ayers, D. F.; Ochsner, U. A.; Janjic, N.; Jarvis, T. C. Inhibition of Methionyl-tRNA Synthetase by REP8839 and Effects of Resistance Mutations on Enzyme Activity. *Antimicrob. Agents Chemother.* **2009**, *53*, 86–94.

- (17) Nallan, L.; Bauer, K. D.; Bendale, P.; Rivas, K.; Yokoyama, K.; Horney, C. P.; Pendyala, P. R.; Floyd, D.; Lombardo, L. J.; Williams, D. K.; Hamilton, A.; Sebt, S.; Windsor, W. T.; Weber, P. C.; Buckner, F. S.; Chakrabarti, D.; Gelb, M. H.; Van Voorhis, W. C. Protein farnesyltransferase inhibitors exhibit potent antimalarial activity. *J. Med. Chem.* **2005**, *48*, 3704–3713.

- (18) Polli, J. W.; Wring, S. A.; Humphreys, J. E.; Huang, L. Y.; Morgan, J. B.; Webster, L. O.; Serabjit-Singh, C. S. Rational use of in vitro P-glycoprotein assays in drug discovery. *J. Pharmacol. Exp. Ther.* **2001**, *299*, 620–628.

- (19) Spencer, A. C.; Heck, A.; Takeuchi, N.; Watanabe, K.; Spremulli, L. L. Characterization of the human mitochondrial methionyl-tRNA synthetase. *Biochemistry* **2004**, *43*, 9743–9754.

- (20) Hirumi, H.; Hirumi, K. Continuous cultivation of *Trypanosoma brucei* blood stream forms in a medium containing a low concentration of serum protein without feeder cell layers. *J. Parasitol.* **1989**, *75*, 985–989.

- (21) Raz, B.; Iten, M.; Grether-Buhler, Y.; Kaminsky, R.; Brun, R. The Alamar Blue assay to determine drug sensitivity of African trypanosomes (*T. b. rhodesiense* and *T. b. gambiense*) in vitro. *Acta Trop.* **1997**, *68*, 139–147.

- (22) Rock, F. L.; Mao, W.; Yaremchuk, A.; Tukalo, M.; Crepin, T.; Zhou, H.; Zhang, Y. K.; Hernandez, V.; Akama, T.; Baker, S. J.; Plattner, J. J.; Shapiro, L.; Martinis, S. A.; Benkovic, S. J.; Cusack, S.; Alley, M. R. An antifungal agent inhibits an aminoacyl-tRNA synthetase by trapping tRNA in the editing site. *Science* **2007**, *316*, 1759–1761.

- (23) Van Voorhis, W. C.; Rivas, K. L.; Bendale, P.; Nallan, L.; Horney, C.; Barrett, L. K.; Bauer, K. D.; Smart, B. P.; Ankala, S.; Hucke, O.; Verlinde, C. L.; Chakrabarti, D.; Strickland, C.; Yokoyama, K.; Buckner, F. S.; Hamilton, A. D.; Williams, D. K.; Lombardo, L. J.; Floyd, D.; Gelb, M. H. Efficacy, pharmacokinetics, and metabolism of

tetrahydroquinoline inhibitors of *Plasmodium falciparum* protein farnesyltransferase. *Antimicrob. Agents Chemother.* **2007**, *51*, 3659–3671.